

RESEARCH PAPER



Ameliorative effects of pyrazinoic acid against oxidative and metabolic stress manifested in rats with dimethylhydrazine induced colonic carcinoma

Anil K. Sahdev^{a,*}, Vinit Raj^{a,*}, Ashok K. Singh^a, Amit Rai^a, Amit K. Keshari^a, Arnab De^b, Amallesh Samanta^b, Umesh Kumar^c, Atul Rawat^{c,d}, Dinesh Kumar^c, Sneha Nath^d, Anand Prakash^d, and Sudipta Saha^a

^aDepartment of Pharmaceutical Sciences, Babasaheb Bhimrao Ambedkar University, Vidya Vihar, Lucknow, India; ^bDepartment of Pharmaceutical Technology, Jadavpur University, Kolkata, West Bengal, India; ^cCentre of Biomedical Research, SGPGIMS Campus, Lucknow, Uttar Pradesh, India; ^dDepartment of Biotechnology, Babasaheb Bhimrao Ambedkar University, Vidya Vihar, Lucknow, India

ABSTRACT

Pyrazinoic acid (PA) is structurally similar to nicotinic acid which acts on G-protein-coupled receptor (GPR109A). GPR109A expresses in colonic and intestinal epithelial sites, and involves in DNA methylation and cellular apoptosis. Therefore, it may be assumed that PA has similar action like nicotinic acid and may be effective against colorectal carcinoma (CRC). CRC was produced via subcutaneous injection of dimethylhydrazine (DMH) at 40 mg/kg body weight once in a week for 4 weeks. After that, PA was administered orally at 2 doses of 10 and 25 mg/kg daily for 15 d to observe the antiproliferative effect. Various physiologic, oxidative stress, molecular parameters, histopathology, RT-PCR and NMR based metabolomics were performed to evaluate the antiproliferative potential of PA. Our results collectively suggested that PA reduced body weight, tumor volume and incidence no. to normal. It restored various oxidative stress parameters and normalized IL-2, IL-6, and COX-2 as compared with carcinogen control. In molecular level, overexpressed IL-6 and COX-2 genes became normal after PA administration. Again, normal tissue architecture was prominent after PA administration. Score plots of PLS-DA models exhibited that PA treated groups were significantly different from CRC group. We found that CRC rat sera have increased levels of acetate, glutamine, o-acetyl-glycoprotein, succinate, citrulline, choline, o-acetyl choline, tryptophan, glycerol, creatinine, lactate, citrate and decreased levels of 3-hydroxy butyrate, dimethyl amine, glucose, maltose, myoinositol. Further the PA therapy has ameliorated the CRC-induced metabolic alterations, signifying its antiproliferative properties. In conclusion, our study provided the evidence that PA demonstrated good antiproliferative effect on DMH induced CRC and thus demonstrated the potential of PA as a useful drug for future anticancer therapy.

ARTICLE HISTORY

Received 27 October 2016
Revised 12 February 2017
Accepted 19 March 2017

KEYWORDS

Colorectal carcinoma; interleukins and COX-2; NMR based metabolomics; oxidative stress; pyrazinoic acid; RT-PCR



Introduction

Colorectal carcinoma (CRC) is considered third most common cancer worldwide and affected 1.4 million people in 2012.¹ It is most challenging scenario for medical practitioners as demand for colon cancer treatment is increasing day to day. Drugs which are used for cancer chemotherapy are relatively toxic in nature and resistance often develops during therapy. Factors responsible for drug resistance involve gene mutation and lesser drug concentration at the site of action.² Synthetic chemotherapeutic agents have been proven good efficacy for CRC treatment, however, researchers achieved very little success due to their chemoresistance.³ Therefore, it is necessary to explore some newer anticancer drugs to save life against CRC.


Pyrazinoic acid (PA) is the metabolite product of pyrazinamide⁴ which is active against *Mycobacterium tuberculosis* in humans.⁵ PA is structurally similar to nicotinic acid. Nicotinic acid acts on G-protein-coupled receptor (GPR109A) which is

expressed in the lumen-facing apical membrane of colonic and intestinal epithelial cells, involves DNA methylation directly or indirectly and induces apoptosis.^{6–8} Therefore, the research question is whether PA produces any action against colon cancer due to structural similarity with nicotinic acid.

To get the answer, PA was administered orally to dimethylhydrazine (DMH) induced colon carcinogenic rats at pre-determined doses. Various oxidative stress parameters, histopathological studies and scanning electron microscopic (SEM) of the colonic tissues were performed to evaluate the protective effect of PA. Enzyme linked immunosorbent assay (ELISA) and real-time quantitative reverse-transcribed polymerase chain reaction (RT-PCR) assays were implemented to elucidate the mechanism of action of PA on the molecular level. Finally, ¹H NMR (nuclear magnetic resonance) based serum metabolic profiling was performed to discover the metabolite modulations in CRC rats after treatment with PA.

CONTACT Sudipta Saha  sudiptapharm@gmail.com  Department of Pharmaceutical Sciences, Babasaheb Bhimrao Ambedkar University, Vidya Vihar, Rai Bareilly Road, Lucknow–226025, India.

*These authors equally contributed to this work.

 Supplemental data for this article can be accessed on the [publisher's website](#).

Results

Estimation of physiologic and biochemical parameters in colon and various enzyme levels in serum

Acute toxicity data revealed that PA had not any toxic manifestation to albino Wistar rats. All biochemical and enzyme levels were normal up to 15 d at 10 and 25 mg/kg doses of PA (data not shown). Various physiologic parameters like body weight, tumor incidence no. and volume, pH and total acidity, were measured during the experiment. The body weight variation was more prominent for group-II (DMH group) and again normalized during drug treatment (Fig. 1A). Similar observation was found out for tumor incidence and volume. Tumor volume decreased up to 4 times as compared with carcinogen group (Fig. 1B and 1C). Fig. 1D and 1E illustrated pH and total acidity of colonic content during cancerous condition. The decrease in colonic pH and increase in total acidity were observed in

carcinogen group (DMH treated group-II) as compared with normal control (group-I). The levels of these parameters were again normalized after oral and intraperitoneal administration of PA and 5-FU (5-fluorouracil), respectively (Fig. 1D and 1E).

Table 1 showed the data for various oxidative stress parameters (SOD, CAT, GSH, TBARS and PC) in colon of all the groups. We observed that there was dramatic reduction of GSH in carcinogen control ($\sim 3.17 \mu\text{M}$) than normal control ($\sim 6.59 \mu\text{M}$). Improvement in GSH level was observed after PA treatment ($\sim 3.76 \mu\text{M}$ for 10 mg/kg and $\sim 3.90 \mu\text{M}$ for 25 mg/kg). Similar trend was observed for SOD, where we found that SOD level decreased to 30–40% in carcinogen control as compared with normal group. This level was again improved up to 90–95% in PA treated groups. The CT enzyme activity was found to be improved for both positive control and treated groups than that of carcinogen control group (Table 1). Further the tissue

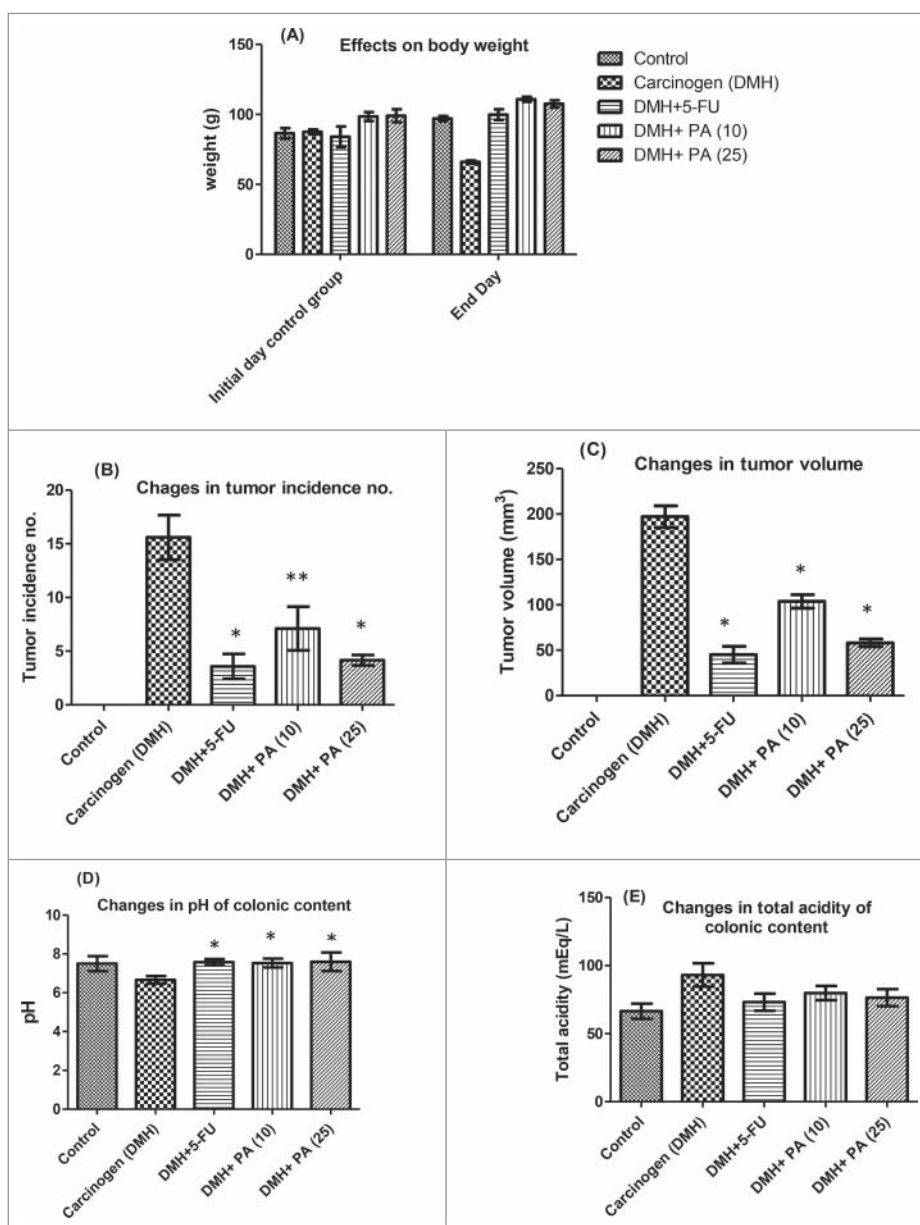


Figure 1. Effects of PA after oral administration of 10 and 25 mg/kg doses for 15 d. Data represented as mean \pm SD (n = 6). Statistically significant differences were observed between carcinogen control and test groups [one way-ANOVA followed by Bonferroni multiple comparison test (**p < 0.01, *p < 0.001)].

Table 1. Effects of PA on oxidative stress parameters in colon after 10 and 25 mg/kg doses for 15 d.

Groups	SOD (U/mg of Protein)	CT mM H ₂ O ₂ decomposed/min/mg of protein	GSH (μ M/mg of Protein)	TBARS (nM of MDA/mg of protein)	PC (μ g/mg of protein)
Control	0.21 \pm 0.02	14.48 \pm 0.72	6.59 \pm 0.24	0.12 \pm 0.02	0.77 \pm 0.46
Carcinogen (DMH)	0.08 \pm 0.07	7.50 \pm 0.44	3.17 \pm 0.29	0.19 \pm 0.01	1.40 \pm 0.29
DMH ⁺ 5-FU	0.20 \pm 0.01*	13.84 \pm 0.58*	5.00 \pm 0.20*	0.13 \pm 0.01*	0.80 \pm 0.19***
DMH ⁺ PA(10)	0.18 \pm 0.03**	8.67 \pm 0.49**	3.76 \pm 0.18**	0.15 \pm 0.02**	0.84 \pm 0.16***
DMH ⁺ PA(25)	0.19 \pm 0.04**	8.95 \pm 0.23*	3.90 \pm 0.14**	0.14 \pm 0.01**	0.82 \pm 0.26***

Data represented as mean \pm SD (n = 6). Statistically significant differences were observed between carcinogen control and test groups [one way-ANOVA followed by Bonferroni multiple comparison test (***p < 0.05, **p < 0.01, *p < 0.001)].

malondialdehyde (MDA) and PC formation was also measured to evaluate the protective action of PA. The MDA formation was \sim 0.19 nM for carcinogen control which was reduced after PA administration (\sim 0.12 nM). Also, the PC formation was higher for carcinogen control (\sim 1.40 μ M) which was reduced to approximately half for PA treated rats (\sim 0.80 μ M) (Table 1). The positive control group (treated with 5-FU) also exhibited significant increase in SOD, CT, GSH levels and significant decrease in PC and MDA levels.

The measurement of serum AST, ALT, LDH and CK was also performed in the similar experiment (Fig. 2). All the enzyme levels were increased up to double as compared with normal during DMH treatment and again back to normal after treatments.

Effect of PA on IL-2, IL-6 and COX-2 levels

Various molecular targets for CRC like IL-2, IL-6, COX-2 and caspase-3 in the colonic tissue were determined during the experiment. We found that all these molecular markers were increased dramatically in the carcinogen control which again normalized after 5-FU and PA treatments (Table 2A). Caspase-3 had no significant role in CRC protection after PA administration (Table 2B).

RT-PCR analysis

RT-PCR analysis was performed to evaluate the gene expression levels of proinflammatory cytokines like IL-6 and COX-2. According to Fig. 3, both IL-6 and COX-2 levels were dramatically increased as compared with normal control. However, these levels became normal after 5-FU

and PA administration. PA action was more prominent at 25 mg/kg dose (Fig. 3).

Histopathology and SEM analysis

Histological changes of colon tissue were observed during DMH treated group as compared with normal. Colorectal tissue showed more vacuolated and damaged cells in DMH group than normal control. PA treatment reduced above histological changes in the colon with respect to carcinogen control (Fig. 4). SEM analysis expressed the similar trends where lesions were less prominent in treated rats as compared with DMH groups (Fig. S1).

NMR based metabolomics

Metabolic effects of PA in DMH rats

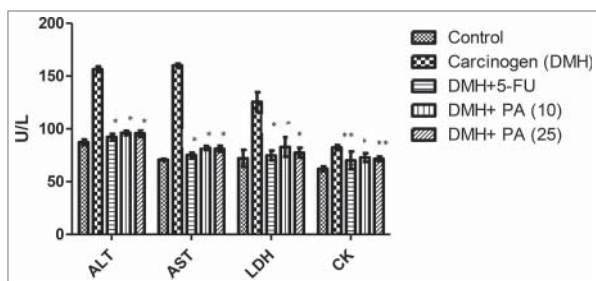
The resulting scaled data sets were introduced into SIMCA-P + 11.0 (Umetrics, Umea, Sweden) where multivariate analyses such as principal components analysis (PCA) and orthogonal partial least-squares-discriminant analysis (OPLS-DA) were performed to investigate and visualize the pattern of metabolite changes in an un-supervised and supervised manner, respectively. PCA was used to authenticate the analytical quality system performance and to observe possible outliers. OPLS-DA was useful to obtain a summary of the complete data

Table 2. Effects of PA on (A) COX-2, IL-2 and IL-6 (B) caspase 3 in colon carcinogenic tissue after oral administration of 10 and 25 mg/kg for 15 d.

(A) Groups	COX-2 (pg/mL)	IL-2 (pg/mL)	IL-6 (pg/mL)
Control	622.69 \pm 63.11	340.84 \pm 71.11	485.14 \pm 75.58
Carcinogen (DMH)	1047.06 \pm 142.24	866.42 \pm 97.41	970.29 \pm 94.05
DMH ⁺ 5-FU	646.15 \pm 23.06*	538.63 \pm 50.00*	542.99 \pm 73.41*
DMH ⁺ PA(10)	848.74 \pm 35.23**	701.90 \pm 41.78**	802.35 \pm 94.05***
DMH ⁺ PA(25)	786.89 \pm 61.02*	700.04 \pm 28.25**	779.96 \pm 81.56**

(B) Groups	Caspase 3 (pg/mL)
Control	75.5 \pm 11.84
Carcinogen (DMH)	50.46 \pm 7.80
DMH ⁺ 5-FU	71.86 \pm 9.04**
DMH ⁺ PA(10)	66.76 \pm 5.80*
DMH ⁺ PA(25)	69.93 \pm 9.72*

Data represented as mean \pm SD (n = 6). Statistically significant differences were observed between carcinogen control and test groups [one way-ANOVA followed by Bonferroni multiple comparison test (***p < 0.05, **p < 0.01, *p < 0.001)].

**Figure 2.** Effect of PA on enzyme levels in plasma after 10 and 25 mg/kg doses for 15 d. Data represented as mean \pm SD (n = 6). Statistically significant differences were observed between carcinogen control and test groups [one way-ANOVA followed by Bonferroni multiple comparison test (*p < 0.001, **p < 0.01)].

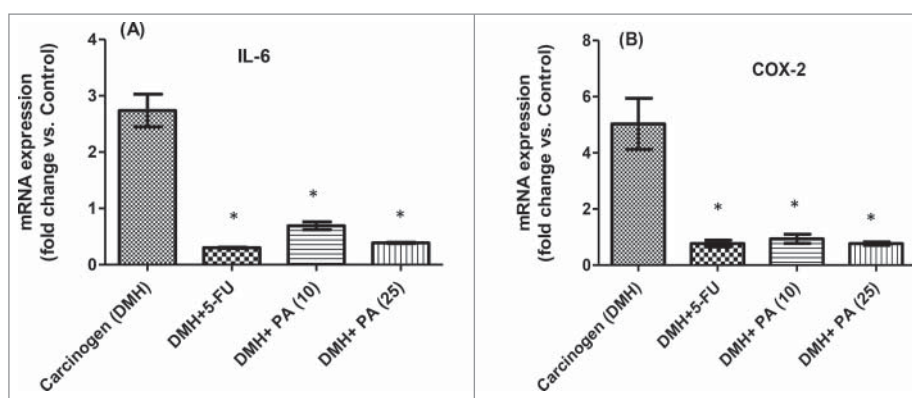


Figure 3. Gene expression levels of proinflammatory cytokines like (A) IL-6 and (B) COX-2 after PA administration in DMH treated rats. Data represented as mean \pm SD (n = 6). Statistically significant differences were observed between carcinogen control and test groups [Paired T-test, (*p<0.001)].

set and to discriminate the variables that are responsible for variation between the groups. The quality of the models was evaluated with the relevant Q^2 and R^2 as well (Fig. 5). The various metabolites were carefully chosen when the statistically major threshold of variable influence on projection (VIP) values achieved from the OPLS-DA model was larger than 1.0. Meanwhile, the p values from a 2-tailed Student's t-test on the regulated peak areas were less than 0.05. Log₂ fold change (FC) was applied to indicate how these particularly different metabolites varied among the groups. The data sets of these differential metabolites were introduced into MetaboAnalyst 3.0 for heat

map generation and multivariate statistics. The areas (AUC) under the receiver operating characteristic curves (ROC) were constructed to evaluate the effectiveness of potential biomarkers. Results were considered significant when p-value is less than 0.05 (Fig. 5, Table 3, Fig. S2).

Metabolic changes during carcinogenic condition with treatments

As depicted in Fig. 5, PLS-DA data showed both the individuals and pairwise analysis revealed $R^2 = 0.90$, $Q^2 \geq 0.59$, indicating the

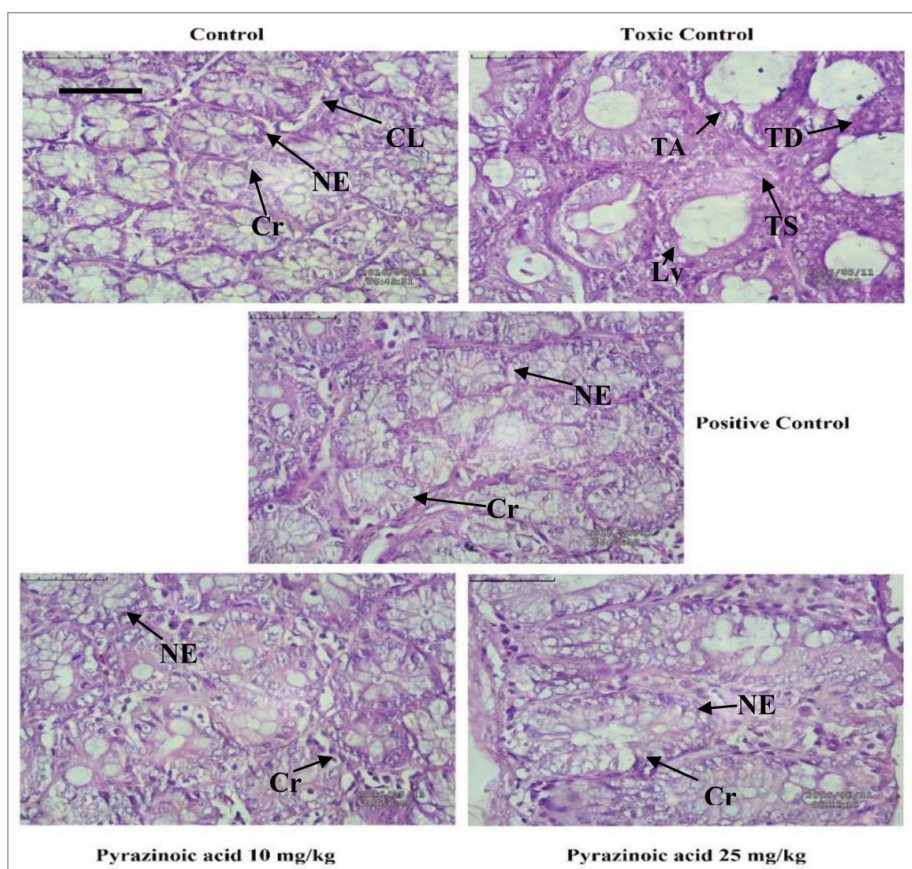


Figure 4. The colonic pathological changes in DMH-induced CC rats (Scale bar 50 μ m). Tumoral vacuoles were prominent in DMH group which was absent after 5-FU and PA administration. (Cr- Crypts, NE- Normal epithelium, CL- Colon lumen, TA- Tubular adenoma, TD- Tumoral deposits, Ly- Lymphatics (lined by endothelium), TS- Tumor stroma).

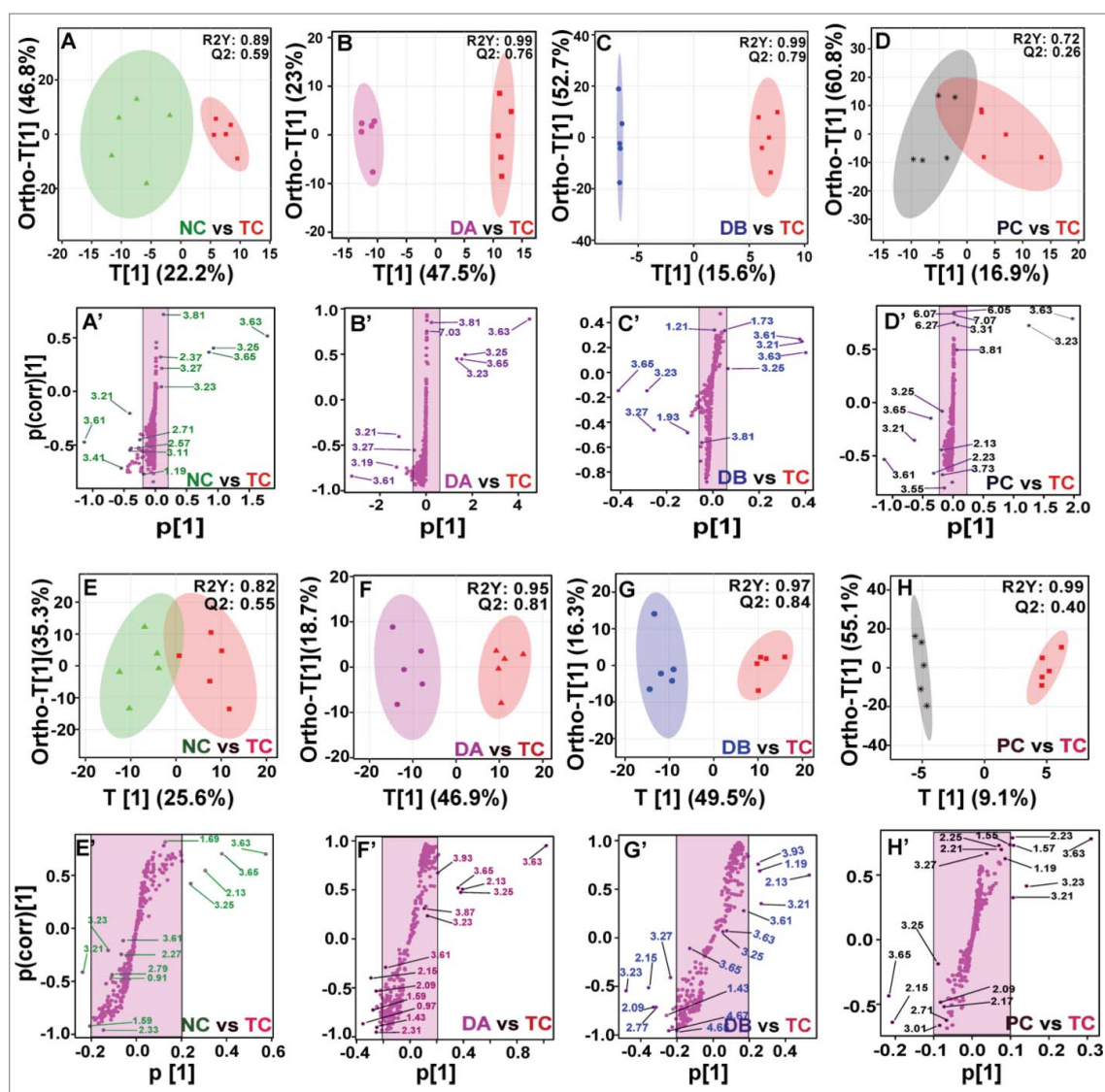


Figure 5. (A-D) OPLS-DA score plots with their respective loading S-plots (A'-D') derived from 1D ^1H CPMG NMR spectra. (E-H) OPLS-DA score plots with their respective loading S-plots (E'-H') derived from 1D DE ^1H NMR spectra. The notions used in the Figure represent respectively: Control (NC), DMH (TC), DMH+5-FU (PC), DMH+PA-10mg (DA) and DMH+PA-25 mg (DB) groups.

significant metabolic changes in colonic rat serum. The key observation of metabolic differences between the control and DMH groups (carcinogen control) along with their chemical shifts (δ), variable importance on projection (VIP) score and p-value are

Table 3. Goodness-of-fit of the PLS-DA models obtained from 1D CPMG and 1D DE of rat serum samples.

Comparison	NMR spectra	R ² Y (cum)	Q ² (cum)	Number of latent variables
Control vs DMH	1D CPMG	0.89	0.59	5
DMH vs DMH +5-FU	1D CPMG	0.72	0.26	5
DMH vs DMH +PA-10 mg	1D CPMG	0.99	0.76	5
DMH vs DMH +PA-25 mg	1D CPMG	0.99	0.79	5
Control vs DMH	1D DE	0.82	0.55	5
DMH vs DMH +5-FU	1D DE	0.99	0.40	5
DMH vs DMH +PA-10 mg	1D DE	0.95	0.81	5
DMH vs DMH +PA-25 mg	1D DE	0.97	0.84	5

listed in Table 4. There were significant increased levels of acetate, glutamine, o-acetyl-glycoprotein, succinate, citrulline, choline, o-acetyl choline, tryptophan, glycerol, creatinine, lactate, citrate and decreased levels of 3-hydroxy butyrate, dimethyl amine, glucose, maltose, myoinositol in DMH treated group (Table 4). All these metabolites became normalized after the administration of PA, particularly at 25 mg/kg dose.

Discussion

PA is only effective against tuberculosis in humans.^{4,5} It is structurally similar to nicotinic acid receptor, (GPR109A) which expressed in epithelial cells of colon or intestine. GPR109A causes DNA methylation and induces apoptosis at the colonic site.⁸ In this study, we investigated the *in vivo* anti-proliferative action of PA via its oral administration to colon carcinogenic albino Wistar rats. The results generated in current study demonstrated the protective effect of PA against DMH-induced CRC and are further discussed in details.

Table 4. Key observed metabolic differences between the healthy control and DMH rat sera. chemical shift, variation, VIP score and p-values of the individual biomarkers are given. *p*-values less than 0.05 were considered as significant. The metabolic differences between DMH and DMH+5-FU, DMH and DMH+PA-10 mg, and DMH and DMH+PA-25 mg have also been presented.

Metabolites	Chemical shift	Variation in DMH with respect to control	VIP	p-value	Variation with respect to DMH		
					5-FU	PA-10 mg	PA-25 mg
3-Hydroxy butyrate	0.88, 1.55, 2.15	↓	1.03	0.04	—	—	—
Acetate	1.92	↑	1.17	0.12	—	↑	↑
Glutamine	2.35	↑	1.49	0.28	↑	↓	↑
O-acetyl-glycoprotein	2.13	↑	1.33	0.26	—	↑	↑
Succinate	2.39	↑	1.09	0.48	↓	—	↓
Citrate	2.52	↑	2.29	0.19	—	↓	↑
Dimethyl amine	2.72	↓	1.50	0.25	↑	↑	↑
Citrulline	2.28	↑	2.19	0.20	—	↓	↑
Choline	3.19	↑	1.51	0.20	—	↓	↓
O-acetyl choline	3.21	↑	1.23	0.17	↑	—	↑
Glucose	3.23–3.92, 4.63, 5.21	↓	3.08	0.08	↑	↑	↓
Maltose	3.25	↓	6.88	0.39	↑	↓	↓
Tryptophan	3.35, 7.18	↑	1.66	0.08	—	↓	—
Glycerol	3.55, 3.65, 3.78	↑	5.93	0.31	↑	↓	↑
Myoinositol	3.27, 3.53, 3.61, 4.06	↓	8.82	0.26	↑	↓	↑
Creatinine	3.03	↑	1.63	0.15	↑	—	↑
Lactate	1.31, 4.11	↑	—	—	↓	↓	↓

Decreased body weight, higher incidence no. and increased tumor volume demonstrated carcinogenic condition in DMH group. These parameters moved to normal after 5-FU and PA administration, protective action was seen after drug administration. There was alteration in pH content and total acidity in carcinogen control, indicating the physiologic changes in colonic cancer condition. After PA treatment, there were an increase in the pH of colonic content and decrease in the total acidity as compared with that of carcinogen control, determining its ability toward non-carcinogenic feature similar to 5-FU. Again, various antioxidant parameters like GSH, SOD, CT were decreased, and MDA, PC were increased in DMH treated rats as compared with that of control group. Alteration of these parameters reflects a good correlation of transformed cells in cancerous condition. The levels of GSH, CT and SOD were restored back to normalcy upon treatment with PA and 5-FU in dose dependent manner. Also the levels of MDA and PC were decreased significantly in PA and 5-FU treated groups, when compared with DMH rats. The restoration of these parameters toward normalcy after the administration of PA could be due to the antioxidant potency of PA to scavenge reactive oxygen species. In addition, various enzymes like ALT, AST, LDH and CK are slightly increased in human serum with liver metastases of colorectal cancer.⁹ Similar observation was recorded in carcinogen control and the levels of all these enzymes were moved to normal after 5-FU and PA treatments, representing the protective effect of PA.

Further histopathology and SEM analysis were performed to find out the morphological changes during DMH administration and drug treatment. Both the analyses revealed that tumoral vacuoles were formed in DMH treated rats. This vacuole formation was vanished in PA and 5-FU groups, demonstrating the protective action of treatments during cancerous condition. In the SEM analysis we found necrotic tissue in DMH treated rats, which was again normalized after PA treatment.

Further, recent investigation suggested that proinflammatory markers like IL-2, IL-6 and COX-2 are generated at colon

cancer site.¹⁰⁻¹² It is well established that COX-2 enzyme is expressed in inflammatory sites, helps in prostaglandins-E2 (PGE2) synthesis which promotes tumor angiogenesis, induces tumor cell growths and inhibits apoptosis. Simultaneously, IL-2 and IL-6 genes are expressed in carcinogenic conditions in colon and these proinflammatory cytokines activate inflammatory cells to transfer signals for the activation of mucosal inflammatory responses and microbial invasion during colon cancer.¹³⁻¹⁶ In consequent with this information, results of ELISA assays suggested that all these inflammatory markers were increased in DMH treated group. Again the concentrations became normalized after the treatment with PA and 5-FU, indicating that PA has anticarcinogenic properties via inhibition of IL-2, IL-6 and COX-2 overexpression at cancer sites.¹⁵ Similar observation had been found out in RT-PCR assays where we found that both IL-6 and COX-2 genes were overexpressed in carcinogenic control. The expression levels was dramatically decreased and came back to normal control after 5-FU and PA administration, again strongly supported the antiproliferative properties of PA in the molecular level particularly at 25 mg/kg dose.^{13,16}

NMR-based serum metabolomics coupled with multivariate statistical analysis were further performed to investigate the CRC-induced metabolic alterations and to evaluate the effect of PA treatment over these alterations. The biologic pathways are involved in the metabolism of these metabolites and their biologic roles were determined by enrichment analysis using MetaboAnalyst.¹⁷ The metabolic pathways closely related to the development of CRC are discussed further. The metabolic pathways involved in this experiment were glycolysis, TCA cycle, phosphatidylinositol, neogluconeogenesis and choline.

The identification of serum biomarkers during CRC condition represents the biochemical pathways altered markedly during cancerous condition. PLS-DA score plot derived from 1D CPMG and 1D DE ¹H NMR spectra of rat serum samples clearly demonstrated the alterations in serum metabolites. The decrease in glucose and increase in

lactate levels in DMH rat serum might be associated with War-burg effect which reflects the higher tissue consumption of glucose during cancer condition, consequently high amount of lactic acid is formed as byproduct.¹⁸ Treatment with 5-FU and PA was resulted into enhanced plasma glucose level due to reduced glucose consumption of cells and thus, protective action of PA was observed. Additionally, the precursor of phosphatidylinositol pathway, myoinositol concentration generally decreases with the development of carcinogenesis in DMH rats. Myoinositol releases phosphate ion in cancerous tissue, increases ATP production and consumption during cell cycle and thus, practically myoinositol concentration reduced in serum.¹⁹ These concentrations again increased via oral administration of PA at 25 mg/kg dose.

On the other hand, elevated concentration of succinate, citrate and glutamine in serum of DMH rats indicated the increase of TCA cycle, followed by glutamate release and increase gluconeogenesis.²⁰ PA administration again decreased all these metabolites concentration, consequently, protective action of PA was again observed against CRC. Furthermore, Marchesi et al. observed lower levels of 3-hydroxy butyrate and dimethyl amine in inflammatory bowel disease due to higher consumption of amino acids by the cancerous tissues.²¹ Similar results had been recognized in NMR based metabolomics with lower levels of amines in DMH treated rats. These metabolites concentration again increased in both the treatment groups. In addition, choline is the major constituent of cell membrane. Metabolomics data showed higher levels of choline and o-acetyl choline in DMH treated rats than normal control. Choline and o-acetyl choline generally help for the synthesis of cell membranes in carcinogenic rats.²² PA administration equalized the choline concentration in our experiment. Overall, PA administration restored all the serum metabolites to normal as compared with DMH treated rats, particularly at 25 mg/kg dose.

Materials and methods

Drugs and reagents

PA, DMH and 2,4-dinitrophenylhydrazine (DNPH) were purchased from Sigma-Aldrich, Bengaluru, India. ALT and AST kits were acquired from the Transasia Biomedicals Pvt. Ltd., Baddi, India. All other chemicals were obtained from Himedia, Mumbai, India. All the solvents and chemicals were of analytical grades with 99% purity and in house distilled water was used throughout the experiment.

Experimental animals

Male albino Wistar rats (80 to 100 g) were used for this experiment and Institutional Animal Ethical Committee approved the protocol previously (Ref no. AEC/PHARM/1601/07/2016/R1). Standard laboratory conditions (temperature $25 \pm 5^\circ\text{C}$ and light/dark cycle of 12 h) were maintained with free access to commercial pellet diet and water *ad libitum*. Animals were kept for one week before experiment.

Acute oral toxicity study

Acute oral toxicity study of PA was performed orally at doses of 10 and 25 mg/kg doses. PA was dissolved in 0.25% carboxymethyl cellulose (CMC) and administered orally to albino Wistar rats for 15 d and the animals were observed every day for any toxic manifestation. Various biochemical parameters in colon (SOD, CT, MDA, PC and GSH) and enzymes levels (ALT, AST, CPK) were measured during experiment.

Experimental design

All animals were randomly divided into 5 groups of 6 animals each ($n = 6$). The groups were then divided as follows: 1st group: 0.25% CMC (2 mL/kg), 2nd group: DMH (40 mg/kg, subcutaneously),^{23,24} 3rd group: DMH+5-FU (10 mg/kg, intraperitoneally), 4th group: DMH+PA (10 mg/kg, orally) and 5th group: DMH+PA (25 mg/kg, orally). The procedure to induce CRC was adopted from literatures, Asfour *et al.* (2014) and Sivaranjani et al. (2016) where it was shown that DMH produced CRC at 40 mg/kg subcutaneous injection, once in a week for 4 weeks to albino Wistar rats. After initial one week of adaptive inhabitation, all rats of group II to V were administered with DMH.

After 28 days, 5-FU and PA were given for 15 d as mentioned above for group III, IV and V. At the end of the experimental period, animals were killed by cervical decapitation and colons were dissected out immediately, rinsed in ice cold saline and stored at -20°C for further studies. The serum was collected, processed and stored for further analysis.

Estimation of various physiologic parameters

Body weight changes were measured at the initial and final days of experiment. Tumor incidence no. was calculated via percentage of animals having tumors. The colons cut with the longitudinal axis, the inner surface was examined macroscopically and tumors of each colon were counted. The length (l), width (w) and height (h) of tumor were measured using a vernier caliper with 0.1 mm graduations, and tumor volume was calculated ($l \times w \times h \times \pi/6$). The pH measurement of colonic content was measured using a pH meter. Total acidity was determined through 0.1N sodium hydroxide (NaOH) using phenolphthalein as indicator in the similar experiment.

Estimation of IL-2, IL-6, COX-2, caspase-3 levels in colonic tissue

Interleukins (IL-2, IL-6) were measured using commercially available ELISA kit from Sigma-aldrich, USA. COX-2 ELISA kit obtained from Bioseps Technology Co., LTD, China. Caspase-3 colorimetric assay kit was procured from Invitrogen Corporation, Camarillo, CA, USA.

Estimation of serum enzyme levels and biochemical estimations in colon

The enzyme levels in serum like aspartate aminotransferase (AST), alanine aminotransferase (ALT), lactate dehydrogenase

(LDH) and creatine phosphokine (CPK) were also measured in serum using commercially available kit from Ebra Diagonosis Pvt. Ltd, Germany. The biochemical parameters like catalase (CT),²⁵ protein carbonyl (PC),²⁶ superoxide dismutase (SOD),²⁷ glutathione (GSH)²⁸ and thiobarbituric acid reactive substances (TBARS)²⁵ were estimated in colon cancer tissue in the similar experiment.

Histopathological studies and scanning electron microscope (SEM) of colon cancer tissues

The procedures adopted for histopathology and SEM were described previously.²⁹

Real-time quantitative reverse-transcribed polymerase chain reaction (RT-PCR) analysis

To determine gene expression, 10 mg of tissue samples of each group was taken in a tube and total RNA was isolated using TriZol reagent and RNeasy mini kit was used to purify the RNA. cDNA was prepared according to the manufacturer's protocol for GeneSure first strand cDNA synthesis kit (Genetix Biotech Asia Pvt. Ltd., New Delhi, India) for RT-PCR. Finally, RT-PCR was performed in Agilent Stratagene Mx3000P series (Applied Biosystems, Foster City, USA) using Sybr[®] green PCR master mix. The mRNA was normalized with housekeeping control β -actin. ΔC_t values were normalized with nontreated control samples for all compounds ($\Delta C_t = C_{t_{\text{gene of interest}}} - C_{t_{\text{housekeeping gene}}}$). Relative changes in the expression level of one specific gene were calculated in terms of $2^{-\Delta\Delta C_t}$ ($\Delta\Delta C_t = \Delta C_{t_{\text{test}}} - \Delta C_{t_{\text{control}}}$).²⁶

The primer sequences were as follows: β -actin, 5'-AAGTCCCTCACCTCCCAAAG-3' (forward) and 5'-AAGCAATGCTGTCACCTTCCC-3' (reverse)³⁰; IL-6, 5'-GCCCTTCAGGAACAGCTATGA-3' (forward) and 5'-TGTCACAACATCAGTCCCAAGA-3' (reverse)³¹; COX-2, 5'-ATCAGAACCGCATTGCCTCT-3' (forward), 5'-GCCAGCAATCTGTCTGTGA-3' (reverse).³²

¹H-NMR based serum metabolic profiling

Sample preparation

All serum samples were liquefied at room temperature. 250 μ L of serum was then mixed with 250 μ L of 0.9% saline sodium-phosphate buffer (strength 50 mM, pH 7.4, prepared in D₂O). The samples were centrifuged at 10,000 rpm for 5 min to remove any precipitates before taking the NMR data. A total 400 μ L of the supernatant sample was used in 5 mm NMR tubes (Wilma Glass, USA) for data acquisition with a co-axial insert containing the known concentration of TSP (Sodium salt of 3-trimethylsilyl-(2,2,3,3-d₄)-propionic acid) i.e. 0.1% was used as external standard to assist metabolite quantification for NMR experiment. Deuterium oxide (D₂O; as a co-solvent and to provide a deuterium field/frequency lock) and sodium salt of TSP were purchased from Sigma-Aldrich, USA.

NMR measurements

All NMR spectra were achieved at 298 K on Bruker Biospin Avance-III 800 MHz NMR spectrometer running at proton

frequency of 800.21 MHz, equipped with CryoProbe and an actively shielded gradient unit with a maximum gradient-strength output of 53 G/cm. The raw NMR data were processed in Topspin-2.1 (Bruker NMR data Processing Software). For each serum sample, one-dimensional ¹H-NMR and diffusion edited ¹H NMR spectra were recorded using the Carr–Purcell–Meiboom–Gill (CPMG) pulse sequence (cpmgrp1d, standard Bruker pulse program) with pre-saturation of the water peak via irradiating it perpetually during the recycle delay (RD) of 5 sec, and the bipolar pulse pair longitudinal eddy current delay (BPP-LED) sequence, respectively. Each CPMG spectrum consisted of the accumulation of 128 scans and lasted for approximately 15 minutes. A total spin–spin relaxation time of 60 ms ($n = 300$ and $2\tau = 200\delta s$) with a line broadening factor of 0.3 Hz was applied to remove broad signals from triglycerides, proteins, cholesterol and phospholipids. A square gradients of 70% of the maximum gradient strength (56 G/cm) and 2 ms duration (followed by a delay of 200 s to allow eddy currents decay) were used for diffusion edited (DE) ¹H NMR pulse sequence. Diffusion time of 120 ms was used to enervate the signals of low molecular weight compounds without affecting the lipid signals. All the spectra were processed using Topspin-2.1 (Bruker NMR data Processing Software) and standard Fourier Transformation (FT) procedure following manual phase and baseline-correction. Prior to FT, each FID was zero-filled to 4096 data points and a sine-bell apodisation function/tapering function was applied. After FT, the chemical shifts were referenced internally to methyl peak of L-lactate (at $\delta = 1.33$ ppm). All the recorded spectra were visually scrutinized for their acceptability and subjected to multivariate statistical analysis to identify the altered metabolic pattern.

Spectral assignment

To identify the distinct allocation of various peaks in the ¹H CPMG NMR spectra, 2-dimensional NMR (2D NMR) spectra were recorded for selected samples including ¹H-¹H total correlation spectroscopy (TOCSY) and ¹H-¹³C heteronuclear single quantum correlation (HSQC). The chemical shifts were identified and assigned at a good extent by comparing them with the chemical shifts available with the software Chenomx 8.1 (Chenomx Inc., Edmonton, Canada). The remaining peaks in the CPMG ¹H NMR spectra were allocated using the previously existing databases available as HMDB (The Human Metabolome Database) and other literature reports.^{33–35}

Multivariate data analysis

The acquired NMR spectra were corrected manually for phase and baseline aberration with Topspin 2.1 (Bruker NMR data Processing Software). The CPMG (δ 0.5–8.5 ppm) and diffusion edited (δ 0.5–5.6 ppm) spectra were then binned into 0.01 ppm wide integrated spectral buckets using AMIX package (Version 3.8.7, Bruker, Bio Spin). The regions containing the resonance from residual water (δ 4.7–5.1 ppm), were excluded to avoid the effects of imperfect water suppression. The binned data were then obtained from AMIX after mean centering and normalization, which was executed by dividing each data point by the sum of all data points present in the sample, to compensate for the differences in concentration of metabolites among individual serum samples.

The data were scaled up using unit variance where identical weight was given to all variables. The resulting data matrices were exported into Microsoft Office Excel 2010 and used for multivariate analysis via open access web-based metabolomic data processing tool, named MetaboAnalyst (<http://www.metabonanalyst.ca/>) and Unscrambler X Software (Version 10.3, CAMO USA, Norway). Principal component analysis (PCA) was first performed on both the CMPG and DE data sets to identify the outliers. To further demonstrate the differences among various groups, supervised partial least squares discriminate analysis (PLS-DA) was performed to identify the metabolites significantly contributing to group differentiation. Model quality was assessed with R^2 , indicating the validity of models against over fitting, and Q^2 , indicating the predictive ability. Potential metabolites markers were extracted from PLS-DA loading plots and the scores of variable importance on projection (VIPs). The statistical significance of these metabolites was calculated by t-test ($p < 0.05$).

Statistical analysis

Statistical analysis was performed using GraphPad Prism 5.0 (San Diego, CA, USA). All results were expressed as mean \pm standard deviation (SD). The data was analyzed by one-way ANOVA (analysis of variances) followed by Bonferroni multiple comparison test. For biochemical estimations, statistical significance differences were considered with respect to D control (* $P < 0.001$, ** $P < 0.01$, *** $P < 0.05$).

Conclusion

In the present study, the protective effect of PA therapy was evaluated on CRC rats by measuring various oxidative stress parameters, pathophysiological enzymes, and using the metabolomics approach. The results collectively suggested that PA normalized various pathophysiological parameters, enzymes and increased antioxidant status demonstrating its anti-oxidant abilities. Morphological studies through histopathology supported that PA maintained normal tissue architecture. In molecular level, PA also normalized IL-2, IL-6 and COX-2 levels. Metabolic profiling confirmed that many metabolites which were significantly altered in DMH treated rats got ameliorated after PA treatment, indicating the anti-proliferative properties of PA for preventing the endogenous metabolic disorders induced by CRC. The possible mechanisms could be related to reinstating the cell membrane damages, improving the energy metabolism, and repairing the inflammation injury. Altogether, the results presented in this study provide the evidence that PA might be effective against DMH treated CRC and could be beneficial for future drug design perspective.

Disclosure of potential conflicts of interest

No potential conflicts of interest were disclosed.

Acknowledgments

Dr. Sudipta Saha would like to express his thanks to the University Grants Commission (UGC), New Delhi, India, for providing UGC-MRP grant [Project no. 42-680/2013(SR)] and Department of Science and Technology

(DST) and Govt. of India (Ref. No. DST/SB/EMEQ-320/2014). We would also like to acknowledge the Department of Medical Education, Govt. of Uttar Pradesh, for supporting the high-field NMR facility at the Center of Biomedical Research, Lucknow, India.

References

- World Health Organisation. Global Cancer Facts & Figures, 2nd Edition, International agency for Research in Cancer. 2008; p 13; <http://oralcancerfoundation.org/wp-content/uploads/2016/03/acspc-027766.pdf>
- Isnard-Bagnis C, Moulin B, Launay-Vacher V, Izzedine H, Tostivint I, Deray G. Renal toxicity of anticancer. *Nephrol Ther* 2005; 1:101-14; PMID:16895673; <https://doi.org/10.1016/j.nephro.2004.12.001>
- Smith BD, Bambach BJ, Vala MS, Barber JP, Enger C, Brodsky RA, Burke PJ, Gore SD, Jones RJ. Inhibited apoptosis and drug resistance in acute myeloid leukaemia. *Brit J Haematol* 1998; 102:1042-9; PMID:9734656; <https://doi.org/10.1046/j.1365-2141.1998.00854.x>
- Weiner IM, Tinker JP. Pharmacology of pyrazinamide: metabolic and renal function studies related to the mechanism of drug-induced urate retention. *J Pharmacol Exp Ther* 1972; 180(2):411-34; PMID:4622054
- Zimic M, Fuentes P, Gilman RH, Gutiérrez AH, Kirwan D, Sheen P. Pyrazinoic acid efflux rate in *Mycobacterium tuberculosis* is a better proxy of pyrazinamide resistance. *Tuberculosis* 2012; 92(1):84-91; PMID:22004792; <https://doi.org/10.1016/j.tube.2011.09.002>
- Lorenzen A, Stannek C, Lang H, Andrianov V, Kalvinsh I, Schwabe U. Characterization of a G protein-coupled receptor for nicotinic acid. *Mol Pharmacol* 2001; 59:349-57; PMID:11160872
- Thangaraju M, Cresci GA, Liu K, Ananth S, Gnanaprakasam JP, Browning DD, Mellinger JD, Smith SB, Digby GJ, Lambert NA, et al. GPR109A Is a G-protein-coupled receptor for the bacterial fermentation product butyrate and functions as a tumor suppressor in colon. *Cancer Res* 2009; 69(7):2826-32; PMID:19276343; <https://doi.org/10.1158/0008-5472.CAN-08-4466>
- Elangovan S, Pathania R, Ramachandran S, Ananth S, Padia RN, Lan L, Singh N, Martin PM, Hawthorn L, Prasad PD, et al. The niacin/butyrate receptor GPR109A suppresses mammary tumorigenesis by inhibiting cell survival. *Cancer Res* 2014; 74(4):1166-78; PMID:24371223; <https://doi.org/10.1158/0008-5472.CAN-13-1451>
- Mielczarek M, Chrzanowska A, Scibior D, Skwarek A, Ashamiss F, Lewandowska K. Arginase as a useful factor for the diagnosis of colorectal cancer liver metastases. *Int J Biol Markers* 2006; 21:40-4; PMID:28207092; <https://doi.org/10.5301/IJBM.2008.4541>
- Al-Sohaily S, Biankin A, Leong R, Kohonen-Corish M, Warusavitarne J. Molecular pathways in colorectal cancer. *J Gastroenterol Hepatol* 2012; 27:1423-31; PMID:22694276; <https://doi.org/10.1111/j.1440-1746.2012.07200.x>
- Mundade R, Imperiale TF, Prabhu L, Loehrer PJ, Lu T. Genetic pathways, prevention, and treatment of sporadic colorectal cancer. *Oncoscience* 2014; 1(6):400-6; PMID:25594038; <https://doi.org/10.18632/oncoscience.59>
- Sano H, Kawahito Y, Wilder RL, Hashiramoto A, Mukai S, Asai K, Kimura S, Kato H, Kondo M, Hla T. Expression of cyclooxygenase-1 and -2 in human colorectal cancer. *Cancer Research* 1995; 55:3785-9; PMID:7641194
- Landi S, Moreno V, Gioia-Patricola L, Guino E, Navarro M, de Oca J, Capella G, Canzian F, Bellvitge Colorectal Cancer Study Group. Association of common polymorphisms in inflammatory genes interleukin (IL)6, IL8, tumor necrosis factor α , NF κ B1, and peroxisome proliferator-activated receptor γ with colorectal cancer. *Cancer Res* 2003; 63:3560-6; PMID:12839942
- Berghella AM, Pellegrini P, Beato TD, Marini M, Tomei E, Adorno D, Casciani CU. The significance of an increase in soluble interleukin-2 receptor level in colorectal cancer and its biological regulating role in the physiological switching of the immune response cytokine network from TH1 to TH2 and back. *Cancer Immunol Immunother* 1998; 45(5):241-9; PMID:9439647; <https://doi.org/10.1007/s002620050439>

15. Coussens LM, Werb Z. A review article Inflammation and cancer. *Nature* 2002; 420:860-7; PMID:12490959; <https://doi.org/10.1038/nature01322>
16. Jung HC, Eckmann L, Yang S-K, Panja A, Fierer J, Morzycka-Wroblewska E, Kagnoff MF. A distinct array of proinflammatory cytokines is expressed in human colon epithelial cells in response to bacterial invasion. *J Clin Invest* 1995; 95:55-65; PMID:7814646; <https://doi.org/10.1172/JCI117676>
17. Xia J, Sinelnikov IV, Han B, Wishart DS. MetaboAnalyst 3.0-making metabolomics more meaningful. *Nucleic Acids Res* 2015; 43:1-7; PMID:25505162; <https://doi.org/10.1093/nar/gku1303>
18. Gribbestad IS, Petersen SB, Fjøsne HE, Kvinnsland S, Krane J. ¹H NMR spectroscopic characterization of perchloric acid extracts from breast carcinomas and non-involved breast tissue. *NMR Biomed* 1994; 7:181-94; PMID:7946996; <https://doi.org/10.1002/nbm.1940070405>
19. Wang H, Wang L, Zhang H, Deng P, Chen J, Zhou B, Hu J, Zou J, Lu W, Xiang P, et al. ¹H NMR-based metabolic profiling of human rectal cancer tissue. *Molecular Cancer* 2013; 12:121; PMID:24138801; <https://doi.org/10.1186/1476-4598-12-121>
20. Lin Y, Ma C, Liu C, Wang Z, Yang J, Liu X, Shen Z, Wu R. NMR-based fecal metabolomics fingerprinting as predictors of earlier diagnosis in patients with colorectal cancer. *Oncotarget* 2016; 7(20): 29454-64; PMID:27107423; <https://doi.org/10.18632/oncotarget.8762>
21. Marchesi JR, Holmes E, Khan F, Kochhar S, Scanlan P, Shanahan F, Wilson ID, Wang Y. Rapid and noninvasive metabonomic characterization of inflammatory bowel disease. *J Proteome Res* 2007; 6:546-51; PMID:17269711; <https://doi.org/10.1021/pr060470d>
22. Kim S, Lee S, Maeng YH, Chang WY, Hyun JW, Kim S. Study of metabolic profiling changes in colorectal cancer tissues using 1D ¹H HR-MAS NMR spectroscopy. *Bull Korean Chem Soc* 2013; 34(5):1467-72; <https://doi.org/10.5012/bkcs.2013.34.5.1467>
23. Asfour W, Almadi S, Haffar L. Thymoquinone suppresses cellular proliferation, inhibits VEGF production and obstructs tumor progression and invasion in the rat model of DMH-induced colon carcinogenesis. *Pharmacol Pharm* 2013; 4:7-17; <https://doi.org/10.4236/pp.2013.41002>
24. Sivaranjani A, Sivagami G, Nalini N. Chemopreventive effect of carvacrol on 1,2-dimethylhydrazine induced experimental colon carcinogenesis. *J Cancer Res Ther* 2016; 12(2):755-62; PMID:27461646; <https://doi.org/10.4103/0973-1482.154925>
25. Lodhi RL, Maity S, Kumar P, Saraf SA, Kaithwas G, Saha S. Evaluation of mechanism of hepatotoxicity of leflunomide using albino wistar rats. *Afr J Pharm Pharmacol* 2013; 17:1625-31; <https://doi.org/10.5897/AJPP2013.3517>
26. Saha S, Chan DSZ, Lee CY, Wong W, New LS, Chui WK, Yap CW, Chan EC, Ho HK. Pyrrolidinediones reduce the toxicity of thiazolidinediones and modify their anti-diabetic and anti-cancer properties. *Eur J Pharmacol* 2012; 697:13-23; PMID:23041271; <https://doi.org/10.1016/j.ejphar.2012.09.021>
27. Kushwaha PS, Raj V, Singh AK, Keshari AK, Saraf SA, Mandal SC, et al. Antidiabetic effects of isolated sterols from *Ficus racemosa* leaves. *RSC Adv* 2015; 5:35230-7; <https://doi.org/10.1039/C5RA00790A>
28. Saha S, New LS, Ho HK, Chui WK, Chan ECY. Direct toxicity effects of sulfo-conjugated troglitazone on human hepatocytes. *Toxicol Lett* 2010; 195:135-41; PMID:20307632; <https://doi.org/10.1016/j.toxlet.2010.03.010>
29. Ong MM, Latchoumycandane C, Boelsterli UA. Troglitazone-induced hepatic necrosis in an animal model of silent genetic mitochondrial abnormalities. *Toxicol Sci* 2007; 97:205-13; PMID:17150972; <https://doi.org/10.1093/toxsci/kfl180>
30. Peinnequin A, Mouret C, Birot O, Alonso A, Mathieu J, Clarénçon D, Agay D, Chancerelle Y, Multon E. Rat pro-inflammatory cytokine and cytokine related mRNA quantification by real-time polymerase chain reaction using SYBR green. *BMC Immunol* 2004; 5:1-10; PMID:14720307; <https://doi.org/10.1186/1471-2172-5-3>
31. Schaefer N, Tahara K, Websky VM, Wehner S, Pech T, Tolba R, Abu-Elmagd K, Kalff JC, Hirner A, Türler A. Role of resident macrophages in the immunologic response and smooth muscle dysfunction during acute allograft rejection after intestinal transplantation. *Transpl Int* 2008; 21:778-91; PMID:18492123; <https://doi.org/10.1111/j.1432-2277.2008.00676.x>
32. Magierowska K, Magierowski M, Hubalewska-Mazgaj M, Adamski J, Surmiak M, Sliwowski Z, Kwiecién S, Brzozowski T. Carbon monoxide (co) released from tricarbonyldichlororuthenium (ii) dimer (dm-2) in gastroprotection against experimental ethanol-induced gastric damage. *PLoS One* 2015; 10:e0140493; PMID:26460608; <https://doi.org/10.1371/journal.pone.0140493>
33. Wishart DS, Jewison T, Guo AC, Wilson M, Knox C, Liu Y, et al. HMDB 3.0-The human metabolome database in 2013. *Nucleic acids Res* 2012; 1-7; PMID: 23161693; <https://doi.org/10.1093/nar/gks1065>
34. Nicholson JK, Foxall PJ, Spraul M, Farrant RD, Lindon JC. 750 MHz ¹H and ¹H-¹³C NMR spectroscopy of human blood serum. *Anal Chem* 1995; 67:793-811; PMID:7762816; <https://doi.org/10.1021/ac00101a004>
35. Guleria A, Bajpai NK, Rawat A, Khetrpal CL, Prasad N, Kumar D. Metabolite characterisation in peritoneal dialysis effluent using high resolution ¹H and ¹H ¹³C NMR spectroscopy. *Magn Reson Chem* 2014; 52:475-9; PMID:24912868; <https://doi.org/10.1002/mrc.4094>